Enhanced terahertz emission by coherent optical absorption in ultrathin semiconductor films on metals

Gopakumar Ramakrishnan,[1,*] **Gopika K. P. Ramanandan,**[1] **Aurèle J. L. Adam,**[1] **Man Xu,**[2] **Nishant Kumar,**[1] **Ruud W. A. Hendrikx,**[3] **and Paul C. M. Planken**[1]

[1]*Optics Research Group, Department of Imaging Science and Technology, Faculty of Applied Sciences, Delft University of Technology, Lorentzweg 1, 2628 CJ Delft, The Netherlands*

[2]*TNO Technical Sciences, Stieltjesweg 1, 2628 CK Delft, The Netherlands*

[3]*Department of Material Science and Engineering, Faculty of Mechanical, Maritime and Materials Engineering (3mE), Delft University of Technology, Mekelweg 2, 2628 CD Delft, The Netherlands*

[*]*G.Ramakrishnan@tudelft.nl*

Abstract: We report on the surprisingly strong, broadband emission of coherent terahertz pulses from ultrathin layers of semiconductors such as amorphous silicon, germanium and polycrystalline cuprous oxide deposited on gold, upon illumination with femtosecond laser pulses. The strength of the emission is surprising because the materials are considered to be bad (amorphous silicon and polycrystalline cuprous oxide) or fair (amorphous germanium) terahertz emitters at best. We show that the strength of the emission is partly explained by cavity-enhanced optical absorption. This forces most of the light to be absorbed in the depletion region of the semiconductor/metal interface where terahertz generation occurs. For an excitation wavelength of 800 nm, the strongest terahertz emission is found for a 25 nm thick layer of amorphous germanium, a 40 nm thick layer of amorphous silicon and a 420 nm thick layer of cuprous oxide, all on gold. The emission from cuprous oxide is similar in strength to that obtained with optical rectification from a 300 μm thick gallium phosphide crystal. As an application of our findings we demonstrate how such thin films can be used to turn standard optical components, such as paraboloidal mirrors, into self-focusing terahertz emitters.

OCIS codes: (300.6495) Spectroscopy, terahertz; (310.6845) Thin film devices and applications; (160.6000) Semiconductor materials.

References and links

1. K. Sakai, ed., *Terahertz Optoelectronics* (Springer-Verlag, Berlin Hiedelberg, 2005).
2. A. J. L. Adam, "Review of Near-Field Terahertz Measurement Methods and Their Applications," J. Infrared Milli. Terahz. Waves **32,** 976–1019 (2011).
3. K. Ezdi, B. Heinen, C. Jördens, N. Vieweg, N. Krumbholz, R. Wilk, M. Mikulics, M. Koch, "A hybrid time-domain model for pulsed terahertz dipole antennas," J. Europ. Opt. Soc. Rap. Public. **4,** 09001 (2009).
4. X.-C. Zhang, J. T. Darrow, B. B. Hu, D. H. Auston, M. T. Schmidt, P. Tham, and E. S. Yang, "Optically induced electromagnetic radiation from semiconductor surfaces," Appl. Phys. Lett. **56,** 2228–2230 (1990).

#189430 - $15.00 USD Received 26 Apr 2013; revised 25 Jun 2013; accepted 25 Jun 2013; published 5 Jul 2013

5. X.-C. Zhang and D. H. Auston, "Optoelectronic measurement of semiconductor surfaces and interfaces with femtosecond optics," J. Appl. Phys. **71,** 326–338 (1992).
6. Y. Jin, X. F. Ma, G. A. Wagoner, M. Alexander, and X.-C. Zhang, "Anomalous optically generated THz beams from metal/GaAs interfaces," Appl. Phys. Lett. **65,** 682–684 (1994).
7. P. Mounaix, A. Younus, J. C. Delagnes, E. Abraham, L. Canioni, M. Fabre, "Spectroscopy and terahertz imaging for sigillography applications," J. Europ. Opt. Soc. Rap. Public. **6,** 11002 (2011).
8. H. Dember, "Photoelectromotive force in cuprous oxide crystals," Phys. Z. **32,** 554-556 (1931).
9. S. Kono, P. Gu, M. Tani, and K. Sakai, "Temperature dependence of terahertz radiation from n-type InSb and n-type InAs surfaces," Appl. Phys. B **71,** 901–904 (2000).
10. M. B. Johnston, D. M. Whittaker, A. Corchia, A. G. Davies, and E. H. Linfield, "Simulation of terahertz generation at semiconductor surfaces," Phys. Rev. B **65,** 165301 (2002).
11. A. Urbanowicz, R. Adomavičius, and A. Krotkus, "Terahertz emission from photoexcited surfaces of Ge crystals," Physica B **367,** 152–157 (2005).
12. A. Urbanowicz, R. Adomavičius, A. Krotkus, and V. L. Malevich, "Electron dynamics in Ge crystals studied by terahertz emission from photoexcited surfaces," Semicond. Sci. Technol. **20,** 1010–1015 (2005).
13. P. Hoyer, M. Theuer, R. Beigang, and E.-B. Kley, "Terahertz emission from black silicon," Appl. Phys. Lett. **93,** 091106 (2008).
14. N. S. Daghestani, S. Persheyev, M. A. Cataluna, G. Ross, and M. J. Rose, "THz generation from a nanocrystalline silicon-based photoconductive device," Semicond. Sci. Technol. **26,** 075015 (2011).
15. M. Li, F. G. Sun, G. A. Wagoner, M. Alexander, and X.-C. Zhang, "Measurement and analysis of terahertz radiation from bulk semiconductors," Appl. Phys. Lett. **67,** 25–27 (1995).
16. X. Mu, Y. J. Ding, K.Wang, D. Jena, and Y. B. Zotova, "Resonant terahertz generation from InN thin films," Opt. Lett. **32,** 1423–1425 (2007).
17. C. T. Que, T. Edamura, M. Nakajima, M. Tani, and M. Hangyo, "Terahertz emission enhancement in InAs thin films using a silicon lens coupler," Jpn. J. Appl. Phys. **50,** 080207 (2011).
18. E. S. Estacio, C. T. Que, F. C. B. Awitan, J. I. Bugante, F. I. de Vera, J. Azares, J. Afalla, J. de Vero, A. S. Somintac, R. V. Sarmago, A. A. Salvador, K. Yamamoto, and M. Tani, "Terahertz emission from indium oxide films grown on MgO substrates using sub-bandgap photon energy excitation," Opt. Express **20,** 4518–4524 (2012).
19. G. Ramakrishnan, "Enhanced terahertz emission from thin film semiconductor/metal interfaces," Ph.D. thesis, Delft University of Technology, The Netherlands (2012).
20. G. Ramakrishnan, R. Chakkittakandy, and P. C. M. Planken, "Terahertz generation from graphite," Opt. Express **17,** 16092–16099 (2009).
21. P. C. M. Planken, H.-K. Nienhuys, H. J. Bakker, and T. Wenckebach, "Measurement and calculation of the orientation dependence of terahertz pulse detection in ZnTe," J. Opt. Soc. Am. B **18,** 313–317 (2001).
22. G. K. P. Ramanandan, G. Ramakrishnan, and P. C. M. Planken, "Oxidation kinetics of nanoscale copper films studied by terahertz transmission spectroscopy," J. Appl. Phys. **111,** 123517 (2012).
23. R. Chakkittakandy, J. A. Corver, and P. C. M. Planken, "Quasi-near field terahertz generation and detection," Opt. Express **16,** 12794–12805 (2008).
24. N. C. J. van der Valk, P. C. M. Planken, A. N. Buijserd, and H. J. Bakker, "Influence of pump wavelength and crystal length on the phase matching of optical rectification," J. Opt. Soc. Am. B **22,** 1714–1718 (2005).
25. R. Chakkittakandy, "Quasi-near field terahertz spectroscopy," Ph.D. thesis, Delft University of Technology, The Netherlands (2010).
26. Y.-P. Yang, W.-Z. Wang, Z.-W. Zhang, L.-L. Zhang, and C.-L. Zhang, "Dielectric and lattice vibrational spectra of Cu_2O hollow spheres in the range of 1–10 THz," J. Phys. Chem. C **115,** 10333-10337 (2011).
27. R. Huber, B. A. Schmid, Y. R. Shen, D. S. Chemla, and R. A. Kaindl, "Stimulated terahertz emission from intraexcitonic transitions in Cu_2O," Phys. Rev. Lett. **96,** 017402 (2006).
28. M. A. Kats, R. Blanchard, P. Genevet, and F. Capasso, "Nanometre optical coatings based on strong interference effects in highly absorbing media," Nat. Mat. **12,** 20–24 (2013).
29. E. Hecht, Optics, 4th ed. (Pearson Education, Inc., San Francisco, 2002).
30. S. Yoshida, "Antireflection coatings on metals for selective solar absorbers," Thin Solid Films, **56,** 321–329 (1979).
31. W. Wan, Y. Chong, Li Ge, H. Noh, A. D. Stone, and Hui Cao, "Time-reversed lasing and interferometric control of absorption," Science **331,** 889–892 (2011).
32. Y. D. Chong, Li Ge, Hui Cao, and A. D. Stone, "Coherent perfect absorbers: time-reversed lasers," Phys. Rev. Lett. **105,** 053901 (2010).
33. K. Kishino, M. Ünlü, J.-I. Chyi, J. Reed, L. Arsenault, and H. Morkoç, "Resonant cavity-enhanced (RCE) photodetectors," IEEE J. Quantum Electron. **27,** 2025–2034 (1991).
34. S. Kasap, and P. Capper, ed. *Springer Handbook of Electronic and Photonic Materials* (Springer Science+Business Media Inc. New York, 2006).
35. G. Klatt, F. Hilser, W. Qiao, M. Beck, R. Gebs, A. Bartels, K. Huska, U. Lemmer, G. Bastian, M. B. Johnston, M. Fischer, J. Faist, and T. Dekorsy, "Terahertz emission from lateral photo-Dember currents," Opt. Express **18,**

#189430 - $15.00 USD Received 26 Apr 2013; revised 25 Jun 2013; accepted 25 Jun 2013; published 5 Jul 2013

4939–4947 (2010).
36. D. L. Staebler and C. R. Wronski, "Reversible conductivity changes in discharge-produced amorphous Si," Appl. Phys. Lett. **31,** 292–294 (1977).
37. A. E. Rakhshani, "Preparation, characteristics and photovoltaic properties of cuprous oxide-a review," Solid-State Electron. **29,** 7–17(1986).
38. A. Parretta, M. K. Jayaraj, A. Di Nocera, S. Loreti, L. Quercia, and A. Agati, "Electrical and optical properties of copper oxide films prepared by reactive RF magnetron sputtering," Phys. Status Solidi A **155,** 399–404 (1996).
39. M. O'Keeffe and W. J. Moore, "Electrical conductivity of monocrystalline cuprous oxide," J. Chem. Phys. **35,** 1324–1328 (1961).
40. F. C. Akkari and M. Kanzari, "Optical, structural, and electrical properties of Cu_2O thin films," Phys. Status Solidi A **207,** 1647–1651 (2010).
41. W. H. Brattain, "The copper oxide rectifier," Rev. Mod. Phys. **23,** 203-212 (1951).
42. V. V. Afanas'ev., *Internal Photoemission Spectroscopy: Principles and Applications* (Elsevier, 2008).
43. J. A. Assimos and D. Trivich, "Photovoltaic properties and barrier heights of single-crystal and polycrystalline Cu_2O-Cu contacts," J. Appl. Phys. **44,** 1687–1693 (1973).
44. Y. Shi, Y. Yang, X. Xu, S. Ma, W. Yan, and L. Wang, "Ultrafast carrier dynamics in Au/GaAs interfaces studied by terahertz emission spectroscopy," Appl. Phys. Lett. **88,** 161109 (2006).
45. S. E. Mani, J. I. Jang, and J. B. Ketterson, "Large third-order susceptibility and third-harmonic generation in centrosymmetric Cu_2O crystal," Opt. Lett. **34,** 2817–2819 (2009).
46. E. Yablonovitch, J. P. Heritage, D. E. Aspnes, and Y. Yafet, "Virtual photoconductivity," Phys. Rev. Lett. **63,** 976–979 (1989).
47. X. Mathew, N. R. Mathews, and P. J. Sebastian, "Temperature dependence of the optical transitions in electrodeposited Cu_2O thin films," Sol. Energ. Mat. Sol. C. **70,** 277–286 (2001).
48. M. E. Toimil Molares, "Fabrication and characterisation of copper nanowires electrochemically deposited in etched ion-track membranes," Ph.D. thesis, Ruperto-Carola University of Heidelberg, Germany (2001).
49. H. Mori, M. Komatsu, K. Takeda, and H. Fujita, "Spontaneous alloying of copper into gold atom clusters," Phil. Mag. Lett. **63,** 173–178 (1991).
50. S. P. Pucic, "Diffusion of copper into gold plating," in Instrumentation and Measurement Technology Conference, 1993. IMTC/93. Conference Record, IEEE, 114–117 (1993).
51. G. K. P. Ramanandan, A. J. L. Adam, G. Ramakrishnan, R. Hendrikx and P. C. M. Planken, "Optical characterization of gold-cuprous oxide interface for terahertz emission applications," in preparation (2013).
52. B. B. Hu, J. T. Darrow, X.-C. Zhang, D. H. Auston, and P. R. Smith, "Optically steerable photoconducting antennas," Appl. Phys. Lett. **56,** 886–888 (1990).
53. R. Chen, N. T. Nuhfer, L. Moussa, H. R. Morris, and P. M. Whitmore, "Silver sulfide nanoparticle assembly obtained by reacting an assembled silver nanoparticle template with hydrogen sulfide gas," Nanotechnology **19,** 455604 (2008).
54. W. Wang, S. Wu, K. Reinhardt, Y. Lu, and S. Chen, "Broadband light absorption enhancement in thin-film silicon solar cells," Nano Lett. **10,** 2012–2018 (2010).

1. Introduction

Ultrafast photoexcitation of semiconductor materials is a commonly used technique to generate broadband terahertz (THz) pulses for imaging and spectroscopy applications [1–3]. THz pulses can be generated from both semiconductor surfaces and from semiconductor/metal interfaces, where a depletion field is present [4–6]. In general, photoexcited charge carriers in the semiconductor drift in the depletion field present near the surface or the interface, resulting in a transient photocurrent which emits THz radiation. THz radiation can also be generated in semiconductors such as indium arsenide (InAs) where the photo-Dember effect can occur [7, 8]. In this case, the incident light pulse creates a strong concentration-gradient of charge carriers. If electrons and holes diffuse away with different speeds, this leads to a transient dipole which can emit a THz pulse [9, 10]. Semiconductors like silicon (Si) and to a lesser extent germanium (Ge) are considered to be bad choices for the optical generation of THz pulses. Si and Ge are indirect-bandgap semiconductors with relatively long carrier lifetimes. Emission of THz pulses from Ge crystal surfaces excited with femtosecond laser pulses was reported by Urbanowicz *et al.* in 2005 [11, 12]. The photo-Dember effect was suggested as the main THz generation mechanism. For crystalline Si, the relatively weak absorption leads to absorption depths which are fairly large, larger than the surface depletion depth. This means that most of

#189430 - $15.00 USD Received 26 Apr 2013; revised 25 Jun 2013; accepted 25 Jun 2013; published 5 Jul 2013

the light gets absorbed in a region of the material where there is no depletion field present and which therefore does not contribute to the emission of THz pulses, in essence wasting optical pump photons. Methods to circumvent this problem have been suggested in the literature. In 2008, Hoyer *et al.* reported THz emission from black Si [13]. Black Si is prepared by surface modification of Si, making the reflectivity low and enhancing the light absorption near the surface. This leads to the emission of stronger THz pulses. THz generation from nano-crystalline Si in a photo-conductive switch was reported in 2011 [14].

In these earlier works, the semiconductors are used either in bulk or as thin films of ~ 1 μm thickness [15–18]. Thin layers of thickness ~ 100 nm or less are not typically used. One of the main reasons for this is the assumption that as the physical thickness becomes smaller than the optical absorption depth, less pump light is absorbed, thus decreasing the emitted THz amplitude.

Here, we report on enhanced THz emission from *ultrathin* layers of a-Si, a-Ge and from poly-Cu_2O deposited on gold (Au). We find that, as the layer becomes much thinner than the optical absorption depth of the pump light, the THz emission increases strongly. For example, for a 25 nm thick layer of a-Ge on Au we measure ~ 7 times stronger fields (~ 49 times higher power) than from a-Ge on glass. For a 40 nm thick layer of a-Si on Au, a bad THz emitter under normal circumstances, we observe the emission of a ~ 42 times larger THz amplitude than from a-Si deposited on glass. We observe a particularly strong emission from ~ 420 nm of poly-Cu_2O on Au excited with laser pulses at a wavelength of 800 nm [19]. The emission amplitude in this case is comparable to the emission by optical rectification from a 300 μm thick, (110) oriented gallium phosphide (GaP) crystal. The strong emission is surprising since the excitation occurs with a photon energy smaller than the bandgap energy of Cu_2O, and also because Cu_2O is not a known THz emitter material.

For all three cases, we find that the THz emission amplitude is related to the optical absorption, which is strongly enhanced by the so called cavity-resonance effect, which causes the semiconductor layer to act as its own antireflection coating. This increases the effective interaction length and concentrates the optical absorption in the depletion region of the material, where it counts for the THz emission. Our results provide a way to turn bad THz emitters into good ones, and as an application we show that we can prepare curved surfaces, such as a paraboloidal mirror, that both emit and concentrate THz light.

2. Experimental

A schematic of the experimental setup is shown in Fig. 1(a) [20]. The laser source (not shown in the figure) is a Ti: Sapphire oscillator (Scientific XL, Femtolasers) generating p-polarized light pulses of 50 fs duration, centered at a wavelength of 800 nm with a repetition rate of 11 MHz. An average pump power of 260 mW is used for exciting the samples. The pump beam is incident on the sample at a 45° angle of incidence. A plano-convex lens of focal length f = 150 mm is used to focus the pump beam to a spot size of $\sim$ 1-2 mm for the case of Cu_2O/Au and a-Ge/Au, and $\sim$ 2-3 mm for the case of a-Si/Au. The emitted THz light is collected using an off-axis paraboloidal mirror of effective focal length f_e = 100 mm and diameter D = 50 mm. Another paraboloidal mirror is used to focus the THz light onto the electro-optic detection crystal, where the probe pulse is also focused. We detect the electric field of the emitted THz pulses by free space electro-optic sampling with a 500 μm thick, (110) oriented zinc telluride (ZnTe) crystal [21]. In some experiments, in order to improve the signal to noise ratio, the pump beam is chopped using a mechanical chopper at a frequency of 3 kHz, and lock-in detection is employed. The integration time used is 300 μs. The detected THz waveforms were typically averaged for about 3 minutes.

The samples consist of stripes of semiconductor layers with a width of about 5 mm and a

#189430 - $15.00 USD Received 26 Apr 2013; revised 25 Jun 2013; accepted 25 Jun 2013; published 5 Jul 2013

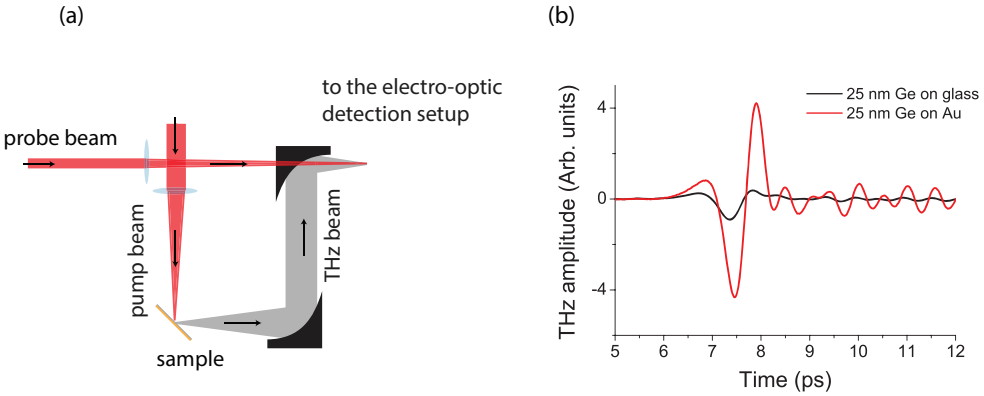

Fig. 1. (a) Schematic of the experimental setup. (b) Measured THz electric field *vs.* time emitted from an a-Ge layer of thickness 25 nm deposited on glass (black), and on Au (red).

length of about 10-20 mm, deposited on Au coated Si substrates. Thin layers of poly-Cu_2O were prepared by first depositing thin films of copper (Cu) using e-beam evaporation, followed by complete oxidation into Cu_2O films by heating at a temperature of 250°C in the ambient atmosphere for three hours. The oxidation of Cu into Cu_2O was confirmed by X-ray diffraction (XRD) measurements. The resulting oxide layer has a thickness $\sim$ 1.5 times larger than the original Cu layer thickness [19,22]. a-Ge and a-Si layers were prepared by radio frequency (RF) plasma sputtering. XRD analysis shows that the sputtered Ge and Si thin films are amorphous in nature.

3. Enhanced terahertz emission from thin films deposited on gold

In Fig. 1(b), we plot the THz electric field as a function of time, emitted from a 25 nm thick a-Ge layer deposited on glass, and from the same thickness of a-Ge deposited on Au. The peak-to-peak THz amplitude emitted from the a-Ge/Au sample is about 7 times larger (about 49 times in intensity) than that from the same thickness of a-Ge deposited on a glass substrate. The emitted THz pulse shown in Fig. 1(b) is p-polarized. It consists of a nearly single-cycle pulse with an oscillatory trailing part that is caused mainly by the absorption and re-emission of the THz light by water vapor in the atmosphere.

In Fig. 2(a), we plot the emitted THz amplitude as a function of layer thickness for a-Ge on glass. As the thickness of the a-Ge layer increases, the emitted THz amplitude is rather small and stays more or less at about the same level. Also plotted in the same figure is the pump light absorption *vs.* a-Ge layer thickness on glass, obtained from the measured incident, reflected, and transmitted pump light from the sample. The overall absorption of the pump light increases as the thickness increases, which is expected as the interaction length of the pump light with a-Ge increases (Lambert-Beer law). It also oscillates as a function of the layer thickness. However, the pump light absorption and the emitted THz amplitude are not simply correlated. In Fig. 2(b), the emitted THz amplitude and the percentage absorption of the pump light are plotted as a function of the thickness of the a-Ge layer deposited on Au. In this case, there is no transmission of the pump light through the sample, as the Au layer blocks the 800 nm beam. Here, the emitted THz amplitude peaks at the values where the pump light absorption also peaks, in contrast with what we saw for the case of a-Ge layers on glass [Fig. 2(a)]. Interestingly, the maximum THz emission occurs when the thickness of the layer is only 25 nm. The next maximum in the emitted THz amplitude, at a thickness of $\sim$ 140 nm, is much smaller than this. We want to

#189430 - $15.00 USD Received 26 Apr 2013; revised 25 Jun 2013; accepted 25 Jun 2013; published 5 Jul 2013

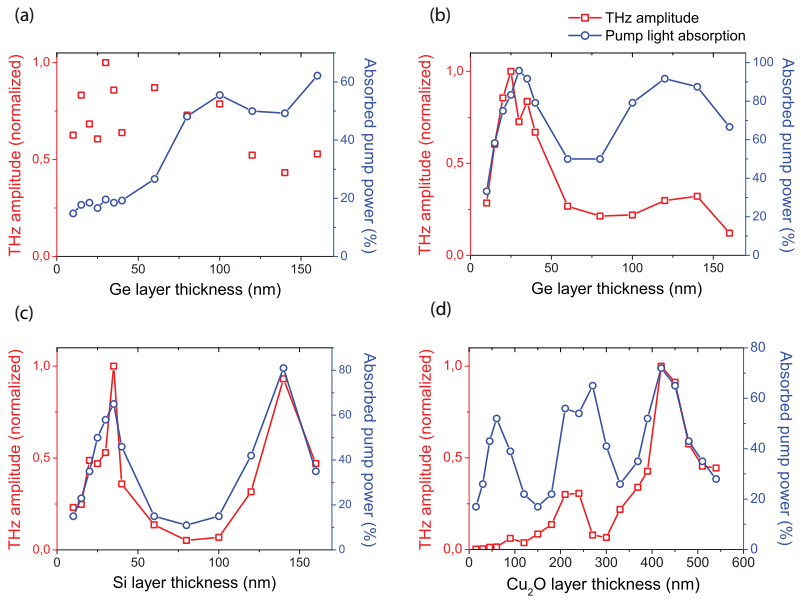

Fig. 2. (a) Measured THz electric field amplitude (red squares) and pump light absorption (blue) as functions of the thickness of a-Ge thin films sputtered on a glass substrate. (b)-(d) Measured THz field amplitude (red) and pump light absorption (blue) as functions of the thickness of the semiconductor ((b) a-Ge, (c) a-Si, (d) poly-Cu_2O) thin films deposited on Au.

point out that the optical absorption at the wavelength of 800 nm, for a layer thickness of 25 nm is surprisingly large, namely $\sim$ 96%.

In Fig. 2(c), the emitted THz amplitude from thin films of a-Si on Au, is plotted as a function of a-Si layer thickness. Maximum THz emission was observed for an a-Si layer thickness of 40 nm. The absorbed pump power is also plotted as a function of the a-Si layer thickness in the same figure. In this case, the pump power absorption increases as the thickness of the layer increases, but the maximum in the emitted THz amplitude coincides with the first pump absorption peak at 40 nm. Although somewhat weaker than for 25 nm of Ge, the optical absorption for such a thin layer is still quite high at $\sim$ 65%, which is slightly lower than the next maximum at a thickness of $\sim$ 140 nm. We find that the THz emission amplitude for 40 nm thick layer of a-Si on Au is $\sim$ 42 times stronger than that from a 40 nm thick a-Si layer on glass, and also much stronger than the emission from bulk Si wafers (not shown here).

In Fig. 2(d), we plot the emitted THz amplitude as a function of the poly-Cu_2O layer thickness on Au. Here the THz amplitude shows an overall increase with the increasing thickness of the film, and oscillates as a function of the layer thickness, as does the absorption of the pump light plotted in the same figure. The biggest surprise here is the absolute strength of the emission. In Fig. 3(a), we show a comparison between the THz amplitudes emitted from a 420 nm thick poly-Cu_2O layer on Au, and from a standard 300 μm thick (110) oriented gallium phosphide (GaP) crystal. Although the signal from GaP is a little stronger, the signals are comparable in magnitude. In Fig. 3(b), we compare the frequency spectra emitted from the three semiconductors on Au, each obtained using the optimum thickness for maximum THz emission (Cu_2O layer of 420 nm thickness, a-Ge layer of 25 nm, and a-Si layer of 40 nm). In this case, a 300 μm thick GaP (110) EO detection crystal was used to maximize the THz detection

#189430 - $15.00 USD Received 26 Apr 2013; revised 25 Jun 2013; accepted 25 Jun 2013; published 5 Jul 2013

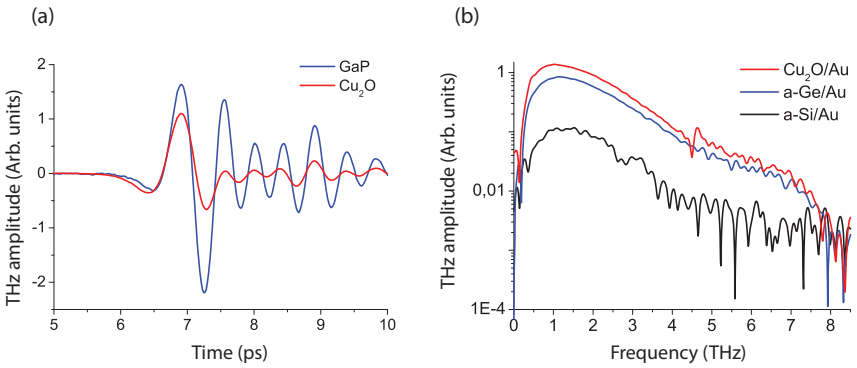

Fig. 3. (a) Measured THz field *vs.* time, emitted from a 300 μm thick GaP (110) crystal (blue), and a 420 nm thick poly-Cu_2O layer deposited on Au (red). (b) Frequency spectra of the THz pulses emitted from a 420 nm Cu_2O layer on 200 nm thick Au (red), 25 nm thick a-Ge layer on 200 nm thick Au (blue) and 40 nm thick a-Si layer on 200 nm thick Au (black). The detection was done in dry-N_2 purged atmosphere, using a 300 μm thick GaP (110) crystal.

bandwidth [23, 24]. In addition, the atmosphere was flushed with dry nitrogen gas (N_2) to reduce the absorption of THz light by water vapor. The three spectra are similar in bandwidth ($\sim$ 7.5 THz) and shape, but different in amplitude, with Cu_2O/Au being the most intense. The comparatively weaker THz emission from a-Si/Au interface could not be recorded with a similar signal-to-noise ratio as for the a-Ge or poly-Cu_2O on Au. This means that for this sample, the higher frequencies $>$ 3.5 THz are barely visible above the noise floor. Interestingly, the spectrum emitted by Cu_2O/Au shows a resonance around 4.5 THz, which corresponds to the lower transverse optical (TO) phonon resonance in crystalline Cu_2O [25, 26]. The resonance is clearly visible in the emission spectrum, even though the Cu_2O layer is only 420 nm thick. We also emphasize that, until now, below-bandgap ultrafast excitation of Cu_2O was not known to lead to the emission of THz radiation. In fact, the only report on the emission of THz light from Cu_2O showed the emission by excitons excited at the bandgap of a high quality single crystal Cu_2O [27]. Here, we observe relatively strong, broadband emission from a 420 nm thick, poly-Cu_2O layer on Au, excited at room temperature, below the bandgap.

The surprisingly strong absorption of light by ultrathin films of semiconductors on top of Au is a recurring feature in our measurements and will be discussed shortly. Based on this observation, we can speculate that the enhanced pump light absorption in such thin layers can perhaps help to explain the observation of enhanced THz emission. In order to understand this more clearly, we need to see how thin absorbing films deposited on metal substrates can show counter-intuitively high absorption of light. In the following sections, we argue that this is most likely explained by the 'coherent optical absorption' or 'cavity-resonance effect' as it is sometimes called. We note that in a recent report, Kats *et al.* also showed that ultrathin films of Ge deposited on metallic substrates can show strong absorption and that they can change the appearance of Au [28].

Interestingly, in Fig. 2(b-d), the peak values in the emitted THz amplitude and in the pump light absorption, plotted as a function of layer thickness, do not show an obvious correlation. In Fig. 2(b), the maximum emitted THz amplitude coincides with the first optical absorption peak at an a-Ge layer thickness of $\sim$ 25 nm. The next peak in the THz amplitude is much smaller, although the optical absorption is comparable to that of the first peak. In the case of a-Si/Au

#189430 - $15.00 USD Received 26 Apr 2013; revised 25 Jun 2013; accepted 25 Jun 2013; published 5 Jul 2013

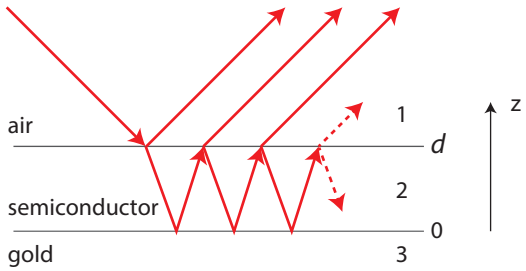

Fig. 4. Reflection of light from a three layer system of media 1, 2 and 3. d is the thickness of the middle layer.

[Fig. 2(c)], the second optical absorption peak at an a-Si layer thickness of 140 nm is higher than the first peak at 40 nm, whereas the emitted THz amplitude is maximum at the first optical absorption peak. For Cu_2O/Au, in Fig. 2(d), the peak values in the emitted THz amplitude increases much more rapidly compared to the peaks in the optical absorption. The reason for these different behaviors stems from the fact that the THz generation basically takes place in the Schottky depletion region. In the case of a-Ge/Au, the extent of the depletion region must be closer to 25 nm. For a-Si/Au, the depletion layer must be about 140 nm thickness, as the THz emission at this thickness is still high compared to the first peak. For Cu_2O/Au, the depletion region must be about 420 nm or wider, as the peak values in the emitted THz amplitude keep increasing with increasing thickness of the Cu_2O layer.

4. Enhanced coherent optical absorption

In Fig. 2, the oscillatory peaks seen in the absorbed pump power as a function of the semiconductor layer thickness are probably the result of the Fabry-Perot oscillations taking place in the thin films. To confirm this, we have performed calculations of the reflection, transmission and absorption of the pump light by these samples.

Considering a three layer system as shown in Fig. 4, the total reflection coefficient r_p can be calculated using the Fresnel equations as, [29]

$$r_p = \frac{r_{12} + r_{23} e^{i2k_{(z,2)}d}}{1 + r_{12} r_{23} e^{i2k_{(z,2)}d}} \tag{1}$$

where r_{12} and r_{23} are the complex reflection coefficients corresponding to the interface between the media 1 and 2, and 2 and 3 respectively, d is the thickness of the semiconductor layer (medium 2), and $k_{(z,2)}$ is the propagation constant in medium 2 along the z axis.

For the cases in which r_{12} becomes equal and opposite in sign to $r_{23} e^{2ik_{(z,2)}d}$, r_p becomes very small. In reality, this means that the first reflected amplitude of light from the interface between media 1 and 2 destructively interferes with the part of the light which gets first reflected from the interface between media 2 and 3 and then emerges from medium 2 [30]. This requires the right value of the imaginary part, κ, of the refractive index of the material, $\tilde{n} = n + i\kappa$, such, that a sufficient number of bounces inside the thin layer 2 can still occur to allow for sufficient destructive interference in the reflected direction. Simultaneously, a significant enhanced absorption occurs due to multiple reflections inside the layer, which effectively increases the optical path length. This effect is somewhat subtle. For a given appropriate thickness of the layer, the absorption coefficient of the semiconductor should have just the right value to make destructive interference in the reflected direction possible, and simultaneously allow for sufficient

#189430 - $15.00 USD Received 26 Apr 2013; revised 25 Jun 2013; accepted 25 Jun 2013; published 5 Jul 2013

absorption during the multiple reflections. If the absorption coefficient is too large, the optical absorption approaches the corresponding bulk values. If the absorption coefficient is too small, most of the light will eventually be reflected, and some of it will be absorbed by the Au underneath. Within the context of photodetection, this enhanced coherent absorption is also known as 'cavity enhanced absorption' and is also related to the recently reported anti-laser [31–33].

5. Terahertz emission from sputtered germanium

In Fig. 5(a), we plot both the measured and the calculated (using Eq. 1) pump light absorption as a function of the a-Ge layer thickness on glass. A good match between the measured and calculated optical absorption is obtained for the complex refractive index $\tilde{n}_{Ge} = 4.5 + i0.6$. A linear increase in the emitted THz amplitude is observed when the pump power incident on the sample is increased (not shown here). This suggests a second-order nonlinear optical process. At least two THz generation mechanisms are possible in this case: the photo-Dember effect and the transient photocurrent surge in the surface depletion field, which are both 'surface-related' phenomena, where with 'surface', we mean a multi-atom thick layer of semiconductor close to the air-semiconductor interface.

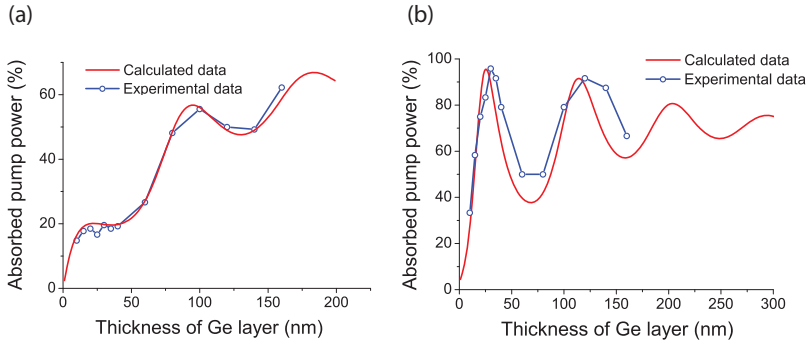

Fig. 5. Measured (blue) and calculated (red) values of pump light absorption plotted as a function of the thickness of the a-Ge layers (a) deposited on glass, (b) deposited on Au.

In Fig. 5(b), we plot the measured and calculated pump power absorption by a-Ge layers deposited on Au, as a function of the layer thickness. The value of the complex refractive index $\tilde{n}$ used for the calculations is the same as in the case of a-Ge layers on glass. The complex refractive index of Au used for the calculations is $\tilde{n}_{Au} = 0.148 + i4.927$. Unlike the behavior seen in the case of a-Ge layers on glass, the absorption by a-Ge/Au does not show an overall increase as the thickness of the a-Ge layer increases. Instead, the maximum absorption occurs at a thickness of 25 nm, and the next etalon peak appearing at 140 nm shows a slightly lower absorption. For thicker layers, the maximum absorption decreases further.

The explanation for this is to be found in a combination of optical absorption and etalon oscillations. Again, we note that this is a subtle effect that depends on the thickness of the layer and the exact value of the absorption coefficient. For example, if the absorption coefficient is very large, no light reaches the Au layer and the a-Ge layer acts like a bulk material with the corresponding values for the reflection and absorption. If the absorption coefficient is too small, interference between the reflection from the air/a-Ge interface and from the a-Ge/Au interface can occur, but most of the light will be reflected anyway or will be absorbed by the Au underneath. In Fig. 6, we show the calculated absorption of p-polarized 800 nm light incident at 45° on a 25 nm thick a-Ge layer on Au, as a function of the absorption index, κ, keeping the

#189430 - $15.00 USD Received 26 Apr 2013; revised 25 Jun 2013; accepted 25 Jun 2013; published 5 Jul 2013

real part of the refractive index, $n = 4.5$, constant. The figure shows that as κ *decreases* from higher values, the absorption *increases* and reaches a maximum at $\kappa = 0.85$. For the complex refractive index used in the calculations shown in Fig. 5, the absorption is at a maximum for an a-Ge layer thickness of 25 nm. For this thickness, enough pump light is back-reflected from the Au to give sufficient destructive interference in the reflected direction. At the same time, multiply-reflected light inside the a-Ge layer leads to an increased effective interaction length and thus to more absorption.

For the case of bulk a-Ge, the attenuation of I_o, the pump light intensity just inside the material (for simplicity, reflection losses are ignored), as a function of the depth z is given by the Lambert-Beer law, [29]

$$I(z) = I_o e^{-\alpha z}. \tag{2}$$

The absorption coefficient α is given by,

$$\alpha = \frac{4\pi\kappa}{\lambda}, \tag{3}$$

where λ is the wavelength of the light wave. The absorption coefficient for a-Ge can be calculated from the imaginary part of the refractive index, using Eq. 3, and has a value of 9.42×10^6 m^{-1}. From this we can calculate, using Eq. 2, that for 96% absorption of the pump light to occur in a *single* pass, a 342 nm thick layer is required. It is remarkable that the same absorption is achieved here by a 25 nm thick layer when it is interfaced with an Au layer. This is ~ 14 times thinner.

It may come as a surprise that the first maximum in the absorption occurs for an a-Ge layer thickness of only 25 nm, whereas for a non-absorbing dielectric coating on a perfect metal, a minimum reflection is obtained when the optical thickness of the coating is $\sim \lambda/4$ (for normal incidence), which corresponds to a thickness of ~ 44 nm. The explanation for this is that, in contrast to reflection by a perfect metal, here the phase-shift of the optical wave upon reflection from the Au is not 180° but has some other value, in effect shifting the position of the first minimum in reflection *vs.* layer thickness to ~ 25 nm. We note that this also implies an increased absorption of light by the metal itself since the a-Ge layer reduces the impedance mismatch between Au and the air. An extreme example of this is the nearly 100% absorption of light at a wavelength of 400 nm by an a-Si layer of only 5 nm thickness deposited on silver (Ag). We observed that this ultrathin layer of a-Si gives Ag an Au-like appearance due to the broadband

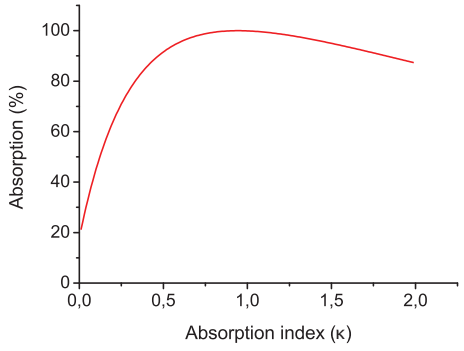

Fig. 6. Calculated percentage absorption of the pump power by a 25 nm thick layer of a-Ge on Au, for 45° angle of incidence, plotted as a function of the absorption index, κ. The real part of the refractive index, $n = 4.5$, is kept fixed.

#189430 - $15.00 USD Received 26 Apr 2013; revised 25 Jun 2013; accepted 25 Jun 2013; published 5 Jul 2013

absorption of light around the wavelength of 400 nm. In [28], something similar was reported for a 7 nm thick layer of Ge on Ag. In terms of maximizing the absorption while reducing the layer thickness, a-Si is therefore a better choice.

5.1. Photocurrent in the Schottky field

So far, we have not discussed the origin of the emitted THz pulses. However, in view of the results it seems likely that a Schottky interface, with a corresponding depletion layer and a static electric field is present near the Au/a-Ge interface. The near infrared pump light centered at the wavelength of 800 nm is absorbed by the a-Ge layer (The bandgap of crystalline Ge is 0.67 eV [34]). This creates electron-hole pairs. The Schottky field at the interface between Au and a-Ge can act on these charge carriers, resulting in a transient photocurrent which can emit a THz pulse into the far field [1].

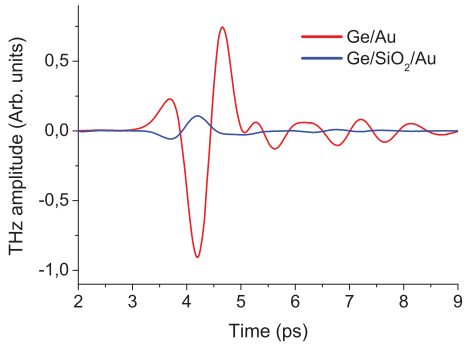

Fig. 7. Measured THz electric field amplitudes as a function of time, emitted from a-Ge/Au (red), and a-Ge/SiO_2/Au (blue).

THz emission, although much weaker, is also seen from a-Ge on glass where no Schottky interface is formed. For crystalline Ge, the photo-Dember effect was reported as the mechanism for the generation of THz pulses [11]. When a concentration gradient is achieved near the surface of a semiconductor by photo-exciting electron-hole pairs, they start diffusing away. If the mobility of the electrons and holes is different, electrons (in general) move faster than holes and leave the holes behind. This leads to the build-up of a dipole layer near the surface. This is known as the photo-Dember field [8,35]. When the excitation of the semiconductor is done with a femtosecond laser pulse, this leads to the generation of a time-varying dipole which can emit a THz pulse. Such a carrier concentration gradient can also form, in principle, when a standing wave is formed by the pump light incident on the sample and the light reflected from the Au layer. Such a standing wave will give rise to a field node at the Au surface with corresponding low intensity. The intensity then increases as the distance to the Au surface increases. In order to determine whether this plays a role, we included a $\sim$ 2 nm thick layer of silicon dioxide (SiO_2) in between a-Ge and Au to form a metal-insulator-semiconductor (MIS) interface. The purpose of this layer is to strongly reduce the possibility of carrier transport between the Au and the a-Ge so as to hinder the formation of a depletion field, while having only a tiny effect on the formation of a standing wave. If the emitted THz amplitude does not change, this can provide evidence that the photo-Dember effect is the dominant generation mechanism. In Fig. 7, we plot the THz electric field as a function of time, emitted from the a-Ge/Au interface and the a-Ge/SiO_2/Au interface. The thickness of the a-Ge layers is 25 nm. The figure shows that the inclusion of the SiO_2 layer reduces the emitted THz amplitude by a factor of about 10. Note also that the sign of the emitted field is flipped. Thus, the photo-Dember effect cannot be the

#189430 - $15.00 USD Received 26 Apr 2013; revised 25 Jun 2013; accepted 25 Jun 2013; published 5 Jul 2013

main mechanism responsible for the strong THz emission from the 25 nm thick a-Ge deposited on the Au surface.

6. Terahertz emission from sputtered silicon

In Fig. 8, we show a comparison of the measured absorbed pump power by a-Si layers on Au *vs.* layer thickness, with the calculated absorbed power. It can be seen that as the thickness of the a-Si layer increases, the absorbed pump power also increases, in reasonable agreement with the experimental results. We can also see the Fabry-Perot oscillations. The refractive index of a-Si in this case is extracted to be $\tilde{n}_{Si} = 3.9 + i0.11$. The absorption coefficient of a-Si can be calculated from Eq. 3 and is 1.7×10^6 m^{-1}. Assuming the same values for bulk a-Si, using Eq. 2, we can calculate that a layer with a thickness of 962 nm is required to achieve 81% of the pump light absorption in a single pass; a value reached here with a layer of only 140 nm thickness deposited on Au. Again, the coherent optical absorption, or the cavity resonance effect, increases the effective optical path length inside the thin a-Si layer, in this case by a factor of $960/140 = 6.9$.

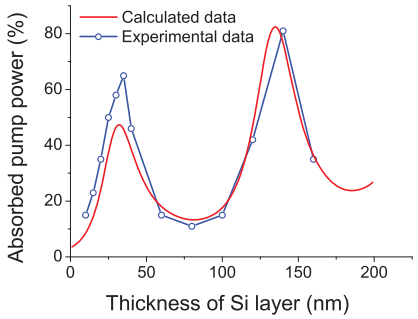

Fig. 8. Measured (blue) and calculated (red) values of pump light absorption plotted as a function of a-Si layer thickness on Au.

Similar to the case of a-Ge/Au, the THz emission from a-Si/Au samples is also through a second-order nonlinear optical process. We note that freshly prepared thin films of a-Si show a photo-stabilization of the THz emission and the emitted THz amplitude drops to about 93% of the original value before reaching a steady level in about 3 minutes [36].

Crystalline Si has a larger bandgap (1.11 eV) compared to Ge [34]. The THz emission from indirect bandgap semiconductors like Si and Ge, is usually small (for Ge) or negligible (for Si). This limits the incorporation of Si and Ge in THz photonic devices. The THz emission from bulk Cu_2O is also very small. However, very thin films of these semiconductors show significant enhancement in THz emission when they are interfaced with Au layers. Various factors can play a role in this process. Based on our experiments, we suggest the enhancement can happen because of three main factors:

- The Schottky field at the semiconductor/Au interface acts as an accelerating field for the photo-generated charge carriers. This can lead to THz emission [1].
- The Au layer acts as a reflector for the forward propagating THz light. The generated THz dipole can radiate in both forward and backward directions, but in the end all THz light emerges in the specular reflection direction.
- As we discussed in detail above, by choosing the thickness of the semiconductor layer appropriately, the pump light can be confined inside a very thin layer close to the Au

#189430 - $15.00 USD Received 26 Apr 2013; revised 25 Jun 2013; accepted 25 Jun 2013; published 5 Jul 2013

surface by the Fabry-Perot cavity resonance, leading to increased optical absorption by the film [33]. This leads to enhanced THz emission because this forces most of the light to be absorbed in a region of the semiconductor, *i.e.* in the Schottky depletion region, where this counts for the THz emission.

7. Terahertz emission from cuprous oxide

Let us now consider THz emission from the poly-Cu_2O/Au interface, which is the best emitter among the three cases, in detail. Normally, Cu_2O is a material which has little absorption at the wavelength of the pump beam, 800 nm. The poly-Cu_2O films that are prepared by the oxidation of Cu layers deposited on glass show a small amount of absorption, probably because of the impurities introduced during the preparation. However for a poly-Cu_2O layer thickness of 60 nm on Au, the optical absorption is already $\sim$ 55%, which increases to 75% as the thickness increases to 420 nm. The oscillations in the absorbed power *vs.* layer thickness are due to etalon effects. The absorption is remarkably high considering that the excitation photon energy is 1.5 eV, which is below the 2.1 eV-bandgap of Cu_2O. In Fig. 9, we show the measured and calculated absorption at 800 nm wavelength as a function of the poly-Cu_2O layer thickness deposited on Au. The refractive index of Cu_2O was adjusted in the calculations to match the peak positions in the calculated curve with those in the experimentally measured curve. This corresponds to a complex refractive index of $\tilde{n}_{Cu_2O} = 2.32 + i0.06$. We note here that this value of the refractive index is different from the reported value of the refractive index of bulk crystalline Cu_2O, which is $\sim 2.7 + i0.06$, perhaps because the poly-Cu_2O we obtain is more porous in nature. For Cu_2O, the resulting absorption coefficient is 9.42×10^5 m^{-1}. Using Eq. 2 we can calculate that for 75% of the light to be absorbed in a single pass, a Cu_2O layer of 1.35 μm thick layer is required, which should be compared with the 420 nm on Au used in the experiment.

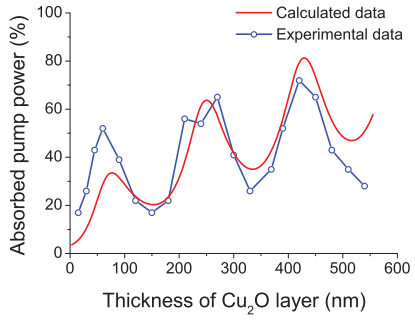

Fig. 9. Measured (blue) and calculated (red) values of pump light absorption plotted as a function of Cu_2O layer thickness on Au.

The increase in the emitted THz amplitude with the thickness of the film can only be expected as long as the film thickness is in the range of the Schottky depletion layer width. Beyond the depletion layer width, the increased absorption by multiple reflections inside Cu_2O may not contribute much to enhanced THz emission, although the pump light absorption still increases. After the 75% absorption achieved at 420 nm thickness, we can assume that more absorption can be achieved at the next peak. However this may not necessarily contribute to higher THz emission from the sample. This is also evidenced by the smaller THz amplitude emitted from the a-Ge layer of $\sim$ 120 nm thickness deposited on Au, although the optical absorption is comparable to that by the layer of 25 nm thickness (Fig. 2(b)). In all the three semiconductors that are used in this study, the exact width of the depletion layer is unknown.

#189430 - $15.00 USD Received 26 Apr 2013; revised 25 Jun 2013; accepted 25 Jun 2013; published 5 Jul 2013

7.1. Terahertz emission mechanism

A linear increase in the emitted THz amplitude from Cu_2O/Au is observed when the pump power incident on the sample is increased (not shown here). This suggests that, here too, a second-order nonlinear optical process is responsible for the emission. Based on our experimental results, there can be three mechanisms responsible, as discussed below. Cu_2O in general is known to be a p-type semiconductor due to the presence of Cu vacancies [37]. Electrical and optical properties of different Cu_2O/metal interfaces have been studied in detail in the past [38–40]. Cu_2O forms a Schottky barrier when it is in contact with metals such as Cu [41]. Ultrafast excitation of a Schottky interface can lead to the formation of transient photocurrents emitting pulses of THz light. In Cu_2O/Cu such a photocurrent can be formed in two different ways: a) By the excitation of sub-bandgap impurity levels in Cu_2O in the depletion region, b) By internal photoemission of holes from the metal into Cu_2O [42–44]. These two processes involve the excitation of real charge carriers. THz emission from a Schottky interface can also arise without the excitation of real charge carriers. The presence of the depletion field can contribute to an effective second-order nonlinearity from the Cu_2O layer, even though crystalline Cu_2O ideally possesses a center of inversion symmetry. A static electric field E_s can break the inversion symmetry to create a field-induced second-order nonlinear susceptibility $\chi^{(2)} \sim E_s\chi^{(3)}$, where $\chi^{(3)}$ is the third-order nonlinear susceptibility [45, 46]. At present, the exact mechanism of THz generation from Cu_2O/Au interfaces is not completely understood. In general, Cu_2O tends to form an Ohmic contact with metals like Au [47] although, recently, some reports have also emerged showing that Au on top of Cu_2O nanowires can form a Schottky contact [48]. It is, however, very likely that a Schottky field is formed in our Cu_2O/Au samples. The reason for this is the formation of a CuAu alloy at the interface. It has been reported that at the elevated temperature used in our experiments to oxidize Cu, Cu atoms can diffuse into Au to form a CuAu alloy at the interface [49, 50]. Since the work function of Cu is lower than that of Au, and since the Cu_2O/Cu interface is known to form a Schottky contact, it is likely that CuAu has a work function lower than that of pure Au, so that a Schottky contact can be more easily formed between Cu_2O and CuAu. Indeed, the chemical removal of the Cu_2O layer from the Au showed that the Au layer has acquired a pink, 'rose-gold' shine, typical for CuAu alloys. XRD analysis of the samples after the removal of Cu_2O layer confirms the presence of the CuAu alloy [51].

8. Terahertz generation from nonplanar surfaces

Thin layers of semiconductors and Au can be prepared on nonplanar surfaces also. This allows us to fabricate optical components that have a double function, such as a mirror that generates and simultaneously focuses the THz radiation. In order to demonstrate this, we prepared a Cu_2O/Au interface on an off-axis paraboloidal mirror surface with f_e = 50 mm and D = 25 mm, by first depositing a 200 nm thick Au layer and then a 150 nm thick Cu layer using e-beam evaporation. The Cu layer was then fully oxidized to Cu_2O by heating it in the atmosphere at 250°C. Now, this paraboloidal mirror surface can act as an extended THz source when illuminated with a pump laser beam covering the mirror surface. A beam with an average pump power of 260 mW is expanded to a diameter of $\sim$ 20 mm on the curved mirror surface. In Fig. 10, we show the schematic of the setup used to generate THz radiation from this paraboloidal mirror. A diverging pump beam from the focus of a smaller focal length plano-convex lens is incident on the paraboloidal mirror surface as shown in the figure. The focus of the pump beam is exactly at the focal point of the paraboloidal mirror. At each point at the surface of the paraboloidal mirror, THz light is generated. The phase relationship of all these THz wavelets is such that the emitted THz beam is plane parallel [52]. This THz beam is focused by another off-axis paraboloidal mirror to the detection crystal. A typical detected THz electric field is shown in

#189430 - $15.00 USD Received 26 Apr 2013; revised 25 Jun 2013; accepted 25 Jun 2013; published 5 Jul 2013

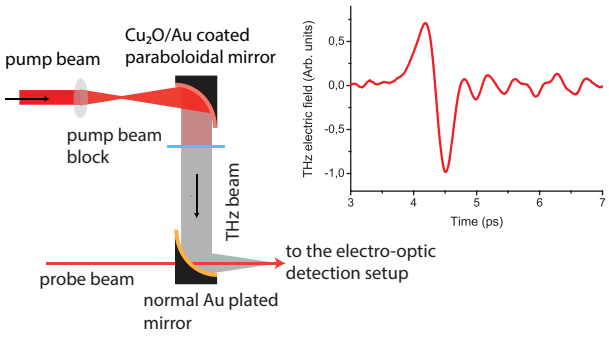

Fig. 10. Schematic of the setup used for the excitation of a Cu_2O coated paraboloidal mirror. Inset: A typical THz electric field *vs.* time, recorded in the setup.

the inset of Fig. 10. This proof-of-principle experiment suggests that (non)planar optical elements in a THz setup can be suitably converted into THz emitters, where the emitted THz beam automatically follows the functionality of the optical element. Generating THz radiation from paraboloidal mirrors themselves can help in reducing the number of optical components used in the optical setup to steer and focus the THz light and to reduce the length of the beam path.

9. Conclusion

In this report, we have demonstrated that, using the method of coherent optical absorption, the THz emission from three semiconductors poly-Cu_2O, a-Ge and a-Si can be significantly enhanced. Our experimental results indicate that the main mechanism responsible for the THz emission in all the three cases is most likely the transient drift of photo-generated charge carriers in the Schottky field. The experiments and calculations show a remarkable, counter-intuitive strong absorption in such thin layers. For poly-Cu_2O, a-Ge and a-Si thin films, the effective optical interaction length increases by a factor of 3, 14 and 7 respectively, when thin layers of these materials are deposited on Au. Thus, significant THz emission from extremely thin layers becomes possible because practically all the charge carriers are generated in the depletion region. In comparison with InAs surface emitters, we estimate that the emitted THz amplitude from Cu_2O/Au is still about a factor of 30 smaller. However, we note that the enhancement of THz emission is not limited to the three semiconductors described in this paper. For example, we also observe fairly strong THz emission from thin films of silver sulfide (Ag_2S), a semiconducting material [53], formed on silver (Ag) substrates. It might also be possible to have enhanced terahertz emission from thin films of GaAs or InAs of the right thicknesses deposited on metal surfaces. Combined with plasmonic enhancements, thin film semiconductor/metal interfaces may be of great value in integrated THz photonic devices [54].

Acknowledgments

The authors thank Prof. Willem Vos of the University of Twente for fruitful discussions, and Dr. Klaas-Jan Tielrooij in the group of Prof. Huib J. Bakker (AMOLF, Amsterdam) for his help during the initial stages of the experiment on nonplanar THz emitting surfaces. P. C. M. P. thanks the Nederlandse Organisatie voor Wetenschappelijk Onderzoek (NWO) and the Stichting voor Technische Wetenschappen (STW) for the financial support in the form of a VICI grant. A. J. L. A. thanks for the financial support in the form of a VENI grant. The financial support from NanoNextNL is also gratefully acknowledged.